Organic & Biomolecular Chemistry

Cite this: *Org. Biomol. Chem.*, 2011, **9**, 4456

www.rsc.org/obc

PAPER

Structure–activity studies of the pelorusides: new congeners and semi-synthetic analogues†

A. Jonathan Singh,[a] Mina Razzak,[b] Paul Teesdale-Spittle,[a] Thomas N. Gaitanos,[a] Anja Wilmes,[a] Ian Paterson,[b] Jonathan M. Goodman,[b] John H. Miller[a] and Peter T. Northcote*[a]

Received 6th December 2010, Accepted 21st March 2011
DOI: 10.1039/c0ob01127d

Two new peloruside congeners (**3** and **4**) were isolated from wild and aquacultured collections of the New Zealand marine sponge *Mycale hentscheli*. Small-scale reactions on peloruside A (**1**) have been performed, which along with the isolation of **3** and **4**, give further insight into the bioactive pharmacophore of **1**.

Introduction

The polyketide macrolide peloruside A (**1**, Fig. 1) was first described in 2000 from the New Zealand marine sponge *Mycale hentscheli* (class Demospongiae, order Poecilosclerida).[1] Interest in the biological properties of **1** has increased significantly recently due to its potential as an anticancer agent. Peloruside A is highly cytostatic and cytotoxic in nanomolar concentrations, and mimics the antimitotic activity of paclitaxel (Taxol®) by arresting cells in the G_2/M phase of the cell cycle by stabilising polymerised microtubules.[2] Peloruside A demonstrates significant biological activity *in vitro* against a number of mammalian cell lines, and is synergistic with paclitaxel and other taxoid site drugs, and competes with laulimalide but not paclitaxel for binding to microtubules.[3–5] Because of its complex molecular architecture and potent biological profile, peloruside A has been the subject of a number of total syntheses.[6–12] We have also recently reported the isolation and total synthesis of peloruside B (**2**), a new potent cytotoxic agent closely related to **1**, isolated from a geographically different specimen of the sponge.[13] Peloruside B showed similar cytotoxic and antimitotic profiles to **1**.

Our efforts to isolate sufficient quantities of peloruside A for further biological studies were facilitated by the aquaculture of sponge collected from Pelorus Sound in the South Island of New Zealand.[14,15] As sponges from this area are known to also produce mycalamide A and pateamine,[15] the result of these large-scale isolations not only allowed us to obtain large amounts of these highly cytotoxic components, but also permitted us to search for other minor compounds of interest. In this article we describe the NMR-directed isolation, structure elucidation and biological activity of two new congeners of peloruside A (**1**), isolated in sub-milligram quantities from wild and aquacultured collections of Pelorus Sound *M. hentscheli*. The isolation of greater quantities of peloruside A also provides entry into synthetic manipulations to the structure that would allow further exploration of the bioactive pharmacophore of this important microtubule-stabilising agent.

[a]*Centre for Biodiscovery, Victoria University of Wellington, Wellington, New Zealand. E-mail: peter.northcote@vuw.ac.nz; Fax: +64 4 463 5237; Tel: +64 4 463 5960*

[b]*University Chemical Laboratory, University of Cambridge, Cambridge, United Kingdom CB2 1EW*

† Electronic supplementary information (ESI) available: NMR data for compounds **5** and **6**, 1D- and 2D-NMR spectra and biological activity data for compounds **1** and **3–6**. See DOI: 10.1039/c0ob01127d

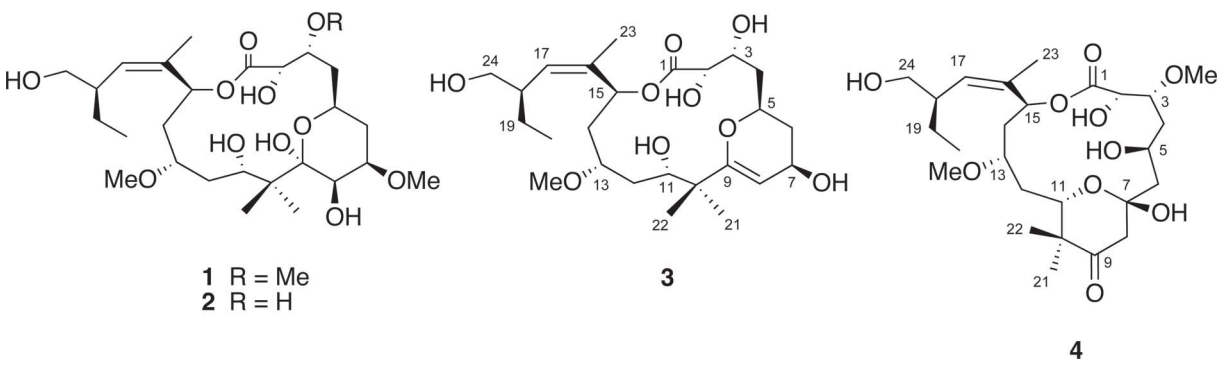

Fig. 1 Structures of pelorusides A–D (**1–4**).

Table 1 ^{13}C (125 MHz) and ^{1}H (500 MHz) NMR data for peloruside C (**3**) in $CDCl_3$

Position	δ_C[a]	mult.	δ_H	mult. (*J*, Hz)	COSY	HMBC	NOESY[c]
1	170.4[b,c]	C	—	—	—	—	
2	76.6	CH	3.98	dd (10.0, 2.0)	3	1[c], 3[c]	3, 4a
3	68.3	CH	4.43	ddd (12.6, 12.6, 2.4)[c]	2, 4a, 4b	—	2, 12b
4a	33.8	CH_2	1.39	m	3, 4b, 5	—	2, 4b, 5
4b			1.75	m	3, 4a	—	4a
5	68.0	CH	4.53	s	4a, 6a, 6b, 7	—	4a, 4b and/or 6a, 6b
6a	29.4	CH_2	1.78	m	5, 6b, 7	—	6b
6b			1.98	m	5, 6a, 7, 8	—	5, 6a, 7
7	64.7	CH	4.41	br d (4.9)[c]	5, 6a, 6b, 8	—	6b, 8
8	92.6	CH	4.77	d (6.5)	6b, 7	6, 7[c], 9	7, 21, 22(w)
9	166.4[b]	C	—	—	—	—	—
10	43.7[b]	C	—	—	—	—	—
11	72.3	CH	4.08	d (10.5)	12a, 12b	12[c], 21[c]	12b, 22
12a	39.0	CH_2	1.35	m	11, 12b	—	12b, 13, 14a, 21
12b			2.07	m	11, 12a	13[c]	3, 11, 12a
13	74.6	CH	3.70	dd (12.1, 6.6)[c]	12a, 12b, 14b	15[c]	12a, 13-OMe, 14a, 14b
13-OMe	58.2	CH_3	3.42	s	—	13	13, 14b, 15, 20
14a	34.6	CH_2	1.98	m	13, 14b, 15	15[c]	12a, 13, 14b
14b			2.05	m	14a	13[c]	13, 14a
15	71.9	CH	5.75	d (10.0)	14a	13[c], 14[c], 17[c], 23[c]	13-OMe, 14a, 14b, 18
16	136.5[b]	C	—	—	—	—	—
17	131.1	CH	5.00	d (10.5)	18, 23	15[c], 23[c]	20, 23, 24a
18	43.2	CH	2.65	m	17, 24a	17[c]	15, 24b
19a	25.0[b]	CH_2	1.16	m	19b, 20	—	19b, 20
19b			1.44	m	19a, 20	17[c]	19a, 20
20	12.3	CH_3	0.89	t (7.5)	19a, 19b	18, 19	17, 19a, 19b
21	16.9	CH_3	1.02	s	22	9 10, 11, 22	8, 12a, 22
22	25.5	CH_3	1.19	s	21	9, 10, 11, 21	8(w), 11, 21
23	18.2	CH_3	1.71	d (1.0)	17	15, 16, 17	17
24a	67.1	CH_2	3.33	td (10.2)	18, 24b, 24-OH	17[c]	17, 24b
24b			3.65	m	24a, 24-OH	20[c]	18, 24a
24-OH	—	—	2.85	s	24a, 24b	—	

[a] Assigned from HSQC data. [b] Assigned from HMBC data. [c] Observed from an impure sample at 600 MHz.

Results and discussion

Peloruside C

A total of 7.5 kg of wild and aquacultured *M. hentscheli* collected from Pelorus Sound, New Zealand was processed to obtain quantities of peloruside A (**1**) for further biological assessment. During the isolation protocol, several compounds with ^{1}H NMR resonances similar to **1** were observed at low levels. A combination of reversed- (PSDVB, Me_2CO/H_2O and $MeOH/H_2O$ gradients) and normal-phase (DIOL, $MeCN/CH_2Cl_2$ and *i*-PrOH/*n*-hexane) column chromatography and HPLC ultimately resulted in the isolation of mycalamide A (266.6 mg), pateamine (18.1 mg), peloruside A (**1**, 85.5 mg), and the two new compounds, pelorusides C (**3**, 130 μg) and D (**4**, 534 μg).

Due to the minute amount of isolated material available, a fully resolved ^{13}C NMR spectrum for peloruside C (**3**) could not be acquired. Instead, protonated carbon shifts were assigned from a multiplicity-edited HSQC experiment, while non-protonated carbons were assigned from long-range proton to carbon correlations in an HMBC experiment (Table 1). Analysis of the positive-ion HRESIMS of **3** established a molecular formula of $C_{25}H_{42}O_9$ (*m/z* 491.2604, $[M - H_2O + Na]^+$, calcd 491.2615), identifying five degrees of unsaturation and an overall difference of $C_2H_6O_2$ from the parent compound **1**. The observation of only one oxymethyl ^{1}H NMR resonance (δ_H 3.42, 13-OMe), rather than the three observed in **1**, accounted for the loss of C_2H_4, leaving the loss of two hydrogen and two oxygen atoms to explain the additional double bond equivalent required by the molecular formula. The HSQC and HMBC spectra of peloruside C (**3**) accounted for all 25 carbon resonances; four methyls (δ_C 12.3; 16.9; 18.2; 25.5), an oxymethyl (δ_C 58.2), five methylenes (δ_C 25.0; 29.4; 33.8; 34.6; 39.0), an oxymethylene (δ_C 67.1), a methine (δ_C 43.2), two olefinic methines (δ_C 92.6; 131.1), seven oxymethines (δ_C 64.7; 68.0; 68.3; 71.9; 72.3; 74.6; 76.6) and four non-protonated centres (δ_C 43.7; 136.5; 166.4; 170.4). The ^{1}H NMR, COSY and HSQC spectra of **3** accounted for 37 hydrogens attached to carbon, leaving the remaining five to be attached to oxygen. The carbon resonance at δ_C 170.4 is typical of an ester carbonyl centre. The quaternary carbon at δ_C 136.5 together with the olefinic methine at δ_C 131.1 is typical of a trisubstituted olefin; whereas, the combination of the other olefinic methine (δ_C 92.6) and the deshielded quaternary carbon at δ_C 166.4 is highly indicative of an enol ether. With three double bonds accounted for, this required that the molecule be a bicyclic system involving two oxygen bridges.

Examination of the COSY and HMBC spectra of peloruside C (**3**) allowed most of the connectivity to be assigned by direct comparison with the parent compound **1** (Table 2). The connectivity of C-1 to C-7 was found to be the same as **1** and **2**. The chemical shifts of methine CH-3 (δ_H 4.43; δ_C 68.3) were similar to **2** (δ_H 4.57; δ_C 69.9) but not **1**, consistent with a free hydroxy group at this position. The chemical shifts of C-5 and C-7 differed substantially from those of both **1** and **2**, suggesting differences in connectivity at these positions. Combined with a

Table 2 ^{13}C (150 MHz) and ^{1}H (600 MHz) NMR data for peloruside A (**1**) in $CDCl_3$ and C_6D_6

		$CDCl_3$			C_6D_6		
Position	mult.	δ_C	δ_H	mult. (J, Hz)	δ_C	δ_H	mult. (J, Hz)
1	C	174.0	—	—	174.2	—	—
2	CH	70.3	4.53	s	71.0	4.79	br d (6.5)
2-OH	—	—	6.75	br s	—	—	
3	CH	78.3	4.22	dd (10.5, 5.5)	78.8	4.36	m
3-OMe	CH_3	56.1	3.31	s	55.2	3.09	s
4a	CH_2	32.6	1.78	m	33.4	1.94	m
4b			2.13	m		2.07	td (11.7, 5.1)
5	CH	63.5	4.25	tdd (11.0, 4.5, 5.5)	64.3	4.37	m
6a	CH_2	31.7	1.53	q (12.0)	32.1	1.69	m
6b			1.78	ddd (12.5, 5.5, 2.5)			
7	CH	75.9	3.82	ddd (11.5, 5.0, 3.0)	76.4	3.95	m
7-OMe	CH_3	55.7	3.38	s	55.9	3.08	s
8	CH	66.8	4.02	d (3.0)	68.0	4.24	d (2.8)
9	C	101.9	—	—	102.4	—	—
10	C	43.6	—	—	44.6	—	—
11	CH	73.9	4.89	br d (10.0)	73.3	4.82	m
11-OH	—	—	4.43	br s			
12a	CH_2	33.9	1.40	d (14.5)	35.6	1.37	m
12b			2.07	ddd (15.0, 11.5, 4.5)		1.73	m
13	CH	77.9	3.99	br d (9.5)	77.6	3.44	m
13-OMe	CH_3	59.1	3.48	s	58.4	3.07	s
14a	CH_2	35.7	2.02	ddd (15.5, 11,5, 1.0)	36.1	1.68	m
14b			2.15	ddd (15.5, 10.0, 1.5)		1.86	ddd (15.7, 9.3, 1.6)
15	CH	70.9	5.68	d (10.5)	71.1	5.80	d (11.1)
16	C	136.1	—	—	136.8	—	—
17	CH	131.1	5.05	d (10.0)	131.2	4.92	d (10.5)
18	CH	43.3	2.61	qt (10.0, 4.0)	43.7	2.73	m
19a	CH_2	24.6	1.17	m	25.1	1.01	m
19b			1.44	m		1.38	m
20	CH_3	12.2	0.85	t (7.5)	12.5	0.83	t (7.4)
21	CH_3	15.8	1.08	s	17.0	1.34	s
22	CH_3	20.8	1.12	s	20.5	1.44	s
23	CH_3	17.5	1.67	d (1.0)	17.8	1.66	d (0.9)
24a	CH_2	66.9	3.36	t (10.5)	67.4	3.50	t (10.1)
24b			3.64	dd (10.5, 4.0)		3.73	m

change in chemical shift in the *gem*-dimethyl region, these indicate changes at C-8 and C-9, which appear as a shielded olefinic methine (δ_H 4.77; δ_C 92.6) and a deshielded olefinic carbon (δ_C 166.4), respectively. The highly polarised nature of the C-8 to C-9 double bond is typical of an enol ether. The C-7 to C-8 connection was evident by a COSY correlation, while the C-9 to C-10 bond was established through HMBC correlations from the C-10 *gem*-dimethyls to C-9 (Fig. 2). In a similar manner to the C-1 to C-7 region, connectivity of the C-11 to C-20 chain was found to be the same as for **1** and **2**. Although no HMBC correlation was observed between H-15 and C-1 to establish the lactone linkage, the chemical shift of H-15 (δ_H 5.75) was consistent with that of an acylated oxymethine. Unfortunately, peloruside C (**3**) degraded before its optical rotation could be measured. The synthetic efforts of De Brabander and Taylor towards *ent*-**1** and **1** respectively noted the inherent instability of a C-7 allylic alcohol.[6,7] It is perhaps the presence of the same moiety in **3** that accounts for its instability.

Determination of the relative stereochemistry of peloruside C (**3**) from NOESY correlations (Table 1) was attempted using the impure sample used to gain additional 2D-NMR data when the original 130 μg sample had degraded. A NOESY correlation between H-2 and H-3, along with the near identical chemical shifts to those of peloruside B (**2**), suggests that the *syn* relative stereochemistry of C-2 and C-3 is conserved from **1**. A transannular NOESY correlation was observed between H-3 and H-12b,

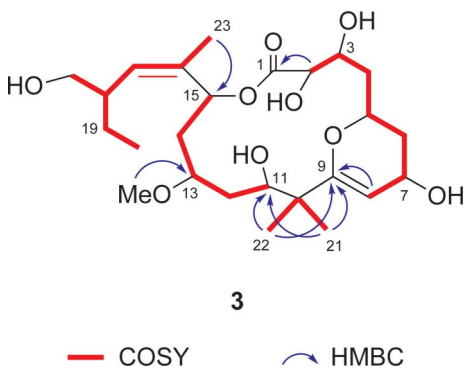

Fig. 2 Key COSY and HMBC correlations for peloruside C (**3**).

indicating a slight conformational change about the C-10 to C-12 region relative to pelorusides A and B, where this across-ring correlation is observed between H-3 and H-11.[1] The downfield methylene proton H-6b was assigned as equatorial on the basis of a w-coupling to the olefinic methine H-8 (Fig. 3). The chemical shifts of CH-15 and the C-16 to C-20 side chain are experimentally close enough to peloruside A to suggest that the relative stereochemistry is retained in this area. Thus, the configuration of each conserved stereocentre of **3** is tentatively assigned as that for peloruside A.

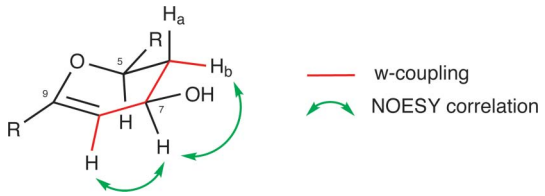

Fig. 3 Key correlations establishing the enol ether moiety of peloruside C (**3**).

Peloruside D

The molecular formula for peloruside D (**4**) was established from HRESIMS as $C_{26}H_{44}O_{10}$ (*m/z* 521.2724, $[M - H_2O + Na]^+$, calcd 521.2721) which revealed five degrees of unsaturation. The ^{13}C NMR, HSQC and HMBC spectra of **4** revealed all 26 carbons of the molecule, while the ^1H NMR and HSQC spectra revealed that 40 of the 44 hydrogens were attached to carbon (Table 3). Two oxymethyl resonances (δ_H 3.48, 3-OMe; δ_H 3.45, 13-OMe) were observed in the ^1H NMR spectrum of **4**, rather than the three present in **1**. Further examination of the NMR data for **4** revealed a saturated ketone resonance at δ_C 216.8, which accounted for the additional degree of unsaturation. Again, construction of subunits from the interpretation of the COSY and HMBC spectra of **4** revealed a high degree of similarity to peloruside A, with the exception of the C-7 to C-11 region. Changes to this area included a hemiacetal C-7 (δ_C 106.0), an isolated methylene CH_2-8 (δ_H 2.01, 2.22; δ_C 35.2) and a saturated ketone C-9 (δ_C 216.8), established in this order through COSY and HMBC correlations. Connectivity of the C-10 *gem*-dimethyl moiety and oxymethine CH-11 (δ_H 4.26; δ_C 82.0) was retained. However, an HMBC correlation from H-11 to the hemiacetal C-7 suggested the presence of an oxygen bridge between C-7 and C-11, leading to the establishment of an unusual, substituted tetrahydro-γ-pyrone moiety (Fig. 4). Connectivity of the C-12 to C-20 chain remained unchanged from peloruside A (**1**).

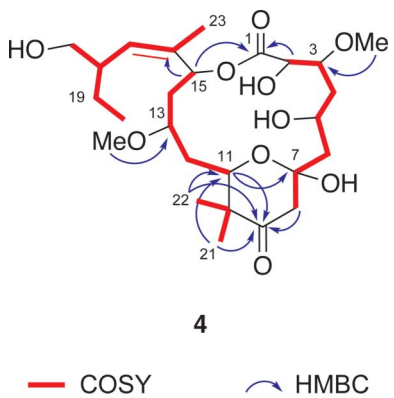

Fig. 4 Key COSY and HMBC correlations for peloruside D (**4**).

As with peloruside C (**3**), assignment of the relative stereochemistry of peloruside D (**4**) was attempted using available ^1H–^1H coupling constants, NOESY correlations (see Table 3) and comparisons with peloruside A (**1**). In the pyrone ring, the upfield methylene proton H-8a was assigned as axial from a NOESY 1,3-diaxial interaction with H_3-22. The NOESY spectrum showed a correlation from H_3-21 (now assigned as equatorial by default) to H-11 (dd, J = 12.0, 1.8 Hz) thus assigning this proton also as equatorial. A strong NOESY correlation was observed between H-2 and H-3, which together with a 7.8 Hz coupling constant for H-2 again suggests that the *syn* relationship of these protons is conserved from the parent molecule **1**. The relative stereochemistry of the C-16 to C-20 side chain of peloruside D was left unaltered as the chemical shifts of this substructure are nearly identical to those of the equivalent region in peloruside A (**1**). From these observations and the assumption that no stereogenic centres have changed in configuration, the relative stereochemistry of peloruside D (**4**) is tentatively assigned as the same as peloruside A (**1**).

Semi-synthetic analogues

We set about performing small scale reactions on peloruside A (**1**) to further explore the bioactive pharmacophore of the compound and to examine the metabolism of the compound in the cell. Peloruside A was subjected to a range of acidic conditions (Table 4) in order to assess the feasibility of semi-synthetic modification of the side chain.[16] Rearrangement and elimination products **5** and **6**, respectively, were formed under different acidic conditions (Fig. 5). These semi-synthetic congeners added further insight into the stability and reactivity of the macrolide. In particular, treatment of **1** with trifluoroacetic acid resulted in compound **5**, while δ-lactone **6** was formed by reaction with triflic acid. Interestingly, **5** is also the only isolated product from the aqueous HCl treatment of peloruside A.

The molecular formula for product **5** was established from the HRESIMS as $C_{26}H_{44}O_{10}$ (*m/z* 521.2731, $[M - H_2O + Na]^+$, calcd 521.2727), revealing five degrees of unsaturation and an overall loss of CH_4O from the parent compound peloruside A (**1**). As in the previous cases, lack of material meant a ^{13}C NMR spectrum was not obtained for this compound. The HSQC and HMBC spectra revealed all the carbons and identified that 40 out of the 44 protons were attached to carbon. The downfield chemical shift of H-15 (δ_H 5.71) and its COSY crosspeak with H-17 (δ_H 4.99) indicated that the macrocycle was intact. The entire backbone of **5** was compiled by interpretation of COSY and HMBC data as had been accomplished previously (Fig. 6). Particular attention was paid to the determination of the C-2 to C-7 region. HMBC correlations from 3-OMe to C-3 and from 13-OMe to C-13 supported the evidence that CH_4O had been lost from the parent compound at position C-7. HMBC correlations from H-2 (δ_H 4.10) to C-1 (δ_C 171.9) and COSY correlations from H-2 through to H_2-7 (δ_H 1.84, 2.17) also showed that C-7 had changed significantly from the parent compound—now appearing as a methylene.

From the HMBC experiment it was evident that H-11 correlated to several carbons (δ_C 215.8; 106.5; 45.5). The methylene protons at position C-7 correlated to the carbon at δ_C 106.5, whereas the methylene protons at position C-6 only correlated to C-5 and C-7. This evidence allowed us to confirm the order of the assignment for the two contiguous methylene pairs. Given that the *gem*-dimethyl group on C-10 shows no correlation to the carbon at δ_C 106.5 but does correlate to the carbon at δ_C 215.8, we propose that loss of methanol at position C-7 gives the enol at position C-8, which tautomerises to the corresponding ketone. The hydroxy group at position C-11 attacks this new C-8 carbonyl to form

Table 3 ^{13}C (150 MHz) and ^{1}H (600 MHz) NMR data for peloruside D (**4**) in $CDCl_3$

Position	δ_C	mult.	δ_H	mult. (*J*, Hz)	COSY	HMBC	NOESY
1	171.6[a]	C	—	—	—	—	—
2	75.6	CH	4.20	d (7.8)	3	1, 3, 4	3, 3-OMe, 4b, 21
3	77.0	CH	3.70	m	2, 4a, 4b	1, 2, 3-OMe, 4, 5	2, 3-OMe, 4b, 6, 15(w), 19b, 20, 23
3-OMe	56.8	CH_3	3.48	s	—	3	2, 3
4a	31.6	CH_2	1.73	m	3	3	4b
4b			2.16	dt (16.2, 3.0)	3, 5	2, 3, 5, 6	2, 3, 4a, 5
5	79.0	CH	4.23	m	4b, 6	—	4b, 6, 8b
6	28.4	CH_2	1.96	m	5, 8a, 8b	5, 7, 8	3, 5, 8b
7	106.0	C	—	—	—	—	—
8a	35.2	CH_2	2.01	m	6, 8b	5, 6, 7	8b, 22
8b			2.22	m	6, 8a	9	5, 6, 8a
9	216.8	C	—	—	—	—	—
10	45.9	C	—	—	—	—	—
11	82.0	CH	4.26	dd (12.0, 1.8)	12a, 12b	7, 9, 10, 13, 22	12a, 13, 13-OMe(w), 21(w), 22
12a	36.7	CH_2	1.36	ddd (13.8, 10.2, 1.8)	11, 12b, 13	—	11, 12b, 13, 21
12b			1.79	m	11, 12a, 13	10, 11	12a, 13, 15, 21
13	74.2	CH	3.77	tt (10.2, 3.0)	12a, 12b, 14a, 14b	—	11, 12a, 12b, 13-OMe, 14a, 14b, 15, 23
13-OMe	57.2	CH_3	3.45	s	—	13	11, 13, 14b
14a	36.1	CH_2	1.42	ddd (14.4, 11.4, 3.1)	13, 14b, 15	—	13, 14b, 15
14b			2.52	ddd (14.4, 11.4, 3.1)	13, 14a, 15	13, 15	13, 14a, 23
15	72.1	CH	5.45	dd (11.4, 3.7)	14a, 14b	1, 13, 14, 16, 17, 23	3(w), 12b, 13, 14a, 17, 18, 20
16	135.7	C	—	—	—	—	—
17	131.6	CH	5.03	d (10.2)	18, 23	15, 18, 19, 23, 24	15, 18, 19a, 19b, 20, 23, 24a, 24b
18	43.0	CH	2.55	m	17,19a, 19b, 24a	16, 17, 18, 19, 24	15, 17, 19a, 19b, 20, 24a, 24b
19a	24.4	CH_2	1.10	m	18, 19b, 20	17, 18, 20, 24	17, 19a, 19b, 20
19b			1.41	m	18, 19a, 20	17, 18, 20, 24	3, 17, 18, 19a, 20
20	12.3	CH_3	0.81	t (7.2)	19a, 19b	18, 19	3, 15, 17, 18, 19a, 19b
21	18.2	CH_3	1.08	s	22	9, 10, 11, 22	2, 11(w), 12a, 12b
22	25.2	CH_3	1.17	s	21	9, 10, 11, 21	8a, 11
23	17.7	CH_3	1.75	d (1.2)	17	15, 16, 17, 19, 24	3, 13, 14b, 17
24a	66.8	CH_2	3.31	t (10.2)	18, 24b	17, 18, 19	17, 18, 19a, 19b, 24b
24b			3.63	dd (10.8, 4.2)	18, 24a	17, 18, 19	15(w), 17, 18, 24a

[a] Assigned from HMBC data.

Table 4 Treatment of peloruside A (**1**) under various acidic conditions[a]

Acid (eq.)	Solvent	Temperature (°C)	Result
PPTS (0.2)	CH_2Cl_2	40[b]	recovered starting material
CSA (0.2)	CH_2Cl_2	40[b]	recovered starting material
Dowex Wx8 (excess)	CH_2Cl_2	40[b]	recovered starting material
$BF_3{\cdot}OEt_2$ (excess)	CH_2Cl_2	20	decomposition
TFA (0.2)	MeOH	20	**5**
TfOH (0.4)	CH_2Cl_2	20	**6**
p-TsOH (0.2)	CH_2Cl_2	20	decomposition

[a] Reaction conditions: acid added to solution of peloruside A (6.1 mmol L^{-1}) at 0 °C, then warmed to noted temperature. [b] Reaction at 20 °C also resulted in recovered starting material.

the five-membered hemiacetal, with concomitant opening of the six-membered hemiacetal native to peloruside A (Scheme 1).[17]

The molecular formula for *seco*-peloruside A δ-lactone (**6**) was established from HRESIMS as $C_{27}H_{48}O_{11}$ (*m/z* 553.2994, $[M - H_2O + Na]^+$, calcd 553.2989), which revealed that it is isomeric with peloruside A. Like peloruside C (**3**), the small amount of material meant a fully resolved ^{13}C NMR spectrum could not be obtained, but the HSQC and HMBC spectra revealed all 27 carbons in the molecule. The HSQC experiment also revealed that 43 of the protons were attached to carbon. Like the parent compound **1**, three oxymethyl resonances (δ_H 3.22, 7-OMe; δ_H 3.14, 3-OMe; δ_H 3.03, 13-OMe) were observed in the ^{1}H NMR spectrum. Further examination and construction of subunits from the interpretation of COSY and HMBC spectra revealed a high degree of similarity to peloruside A. A series of COSY and HMBC correlations established the same linear sequences for the C-1 to C-8 and C-11 to C-20 regions (Fig. 7). The two subunits were joined together through HMBC correlations from the C-10 *gem*-dimethyl moiety to C-9 (now a saturated ketone at δ_C 215.3) and C-11, and from H-8 to C-9. With the carbon connectivity

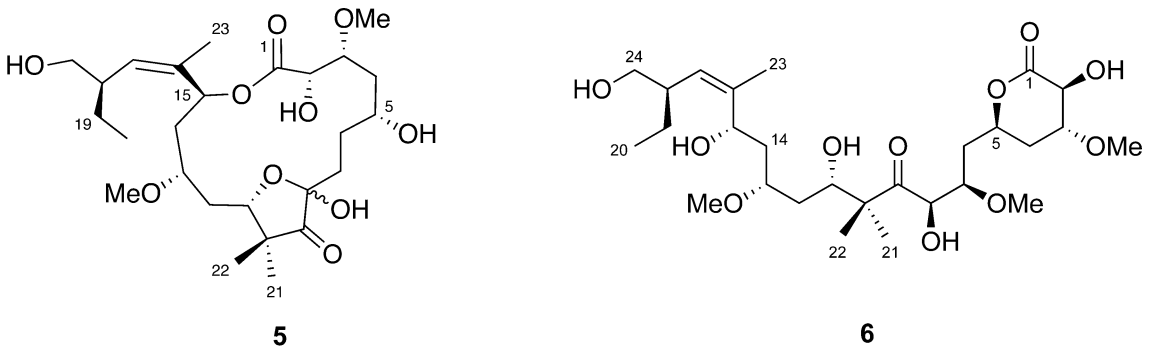

Fig. 5 Semi-synthetic analogues formed from acidic treatment of peloruside A (**1**).

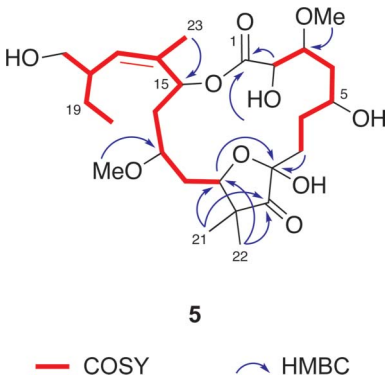

Fig. 6 Key COSY and HMBC correlations for compound **5**.

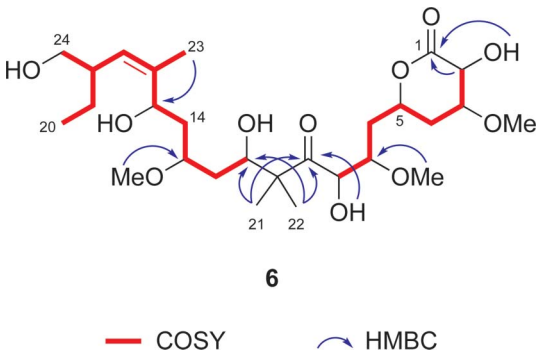

Fig. 7 Key COSY and HMBC correlations for δ-lactone **6**.

accounted for, differences in functionality at positions CH-5 and CH-15 were evident. When the NMR spectra of **1** is taken in C_6D_6 (Table 2), these positions appear at δ_H 4.37, δ_C 64.3 and δ_H 5.80, δ_C 71.1 respectively. With compound **6**, the chemical shifts of CH-5 (δ_H 4.62; δ_C 72.1) and CH-15 (δ_H 3.96; δ_C 73.9) clearly show where the changes in functionality have occurred, which suggests hydrolysis of the macrolide and re-lactonisation about C-5. The CH-5 position in compound **5** also points to a significant change in the equivalent position of **6**.

The chemical shift and coupling pattern of the methylene protons at position C-4 were typical of protons in a six-membered boat-like conformation that the δ-lactone could be expected to form (Fig. 8). Characteristically, the pseudoaxial proton H-4a (δ_H

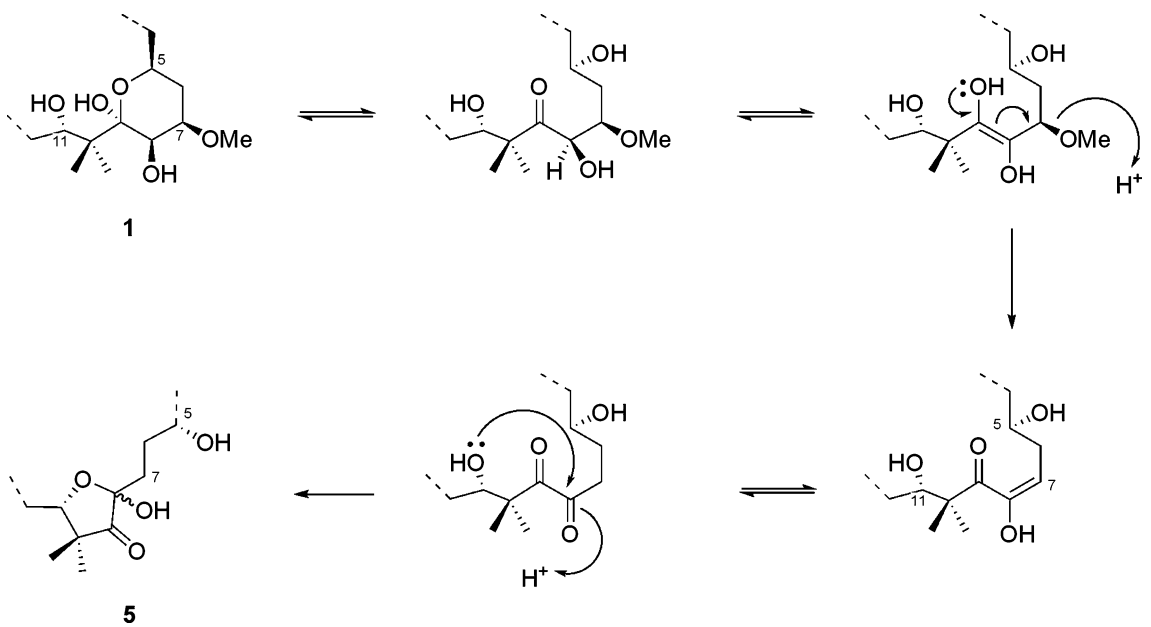

Scheme 1 Proposed acid-catalysed formation of compound **5** from peloruside A (**1**).

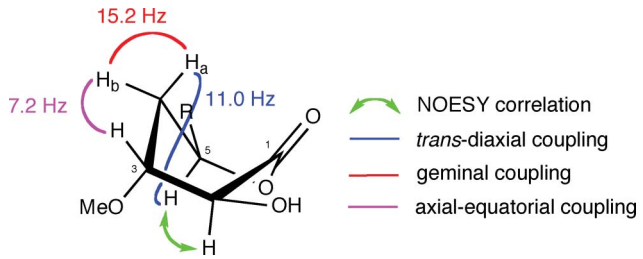

Fig. 8 Key correlations establishing the δ-lactone moiety of compound **6**.

1.24) is upfield from the pseudoequatorial proton H-4b (δ_H 1.50). Consistent with the proposed substitution of the δ-lactone, based on the stereochemistry of peloruside A, H-4a exhibited a large geminal coupling to H-4b and a large *trans*-diaxial coupling to H-5. Similarly, H-4b showed a large geminal coupling to H-4a and two small equatorial-axial couplings to H-3 and H-5, consistent with the bond angles of the proposed structure. Additionally, the observation of a NOESY correlation between H-2 and H-5, which is not apparent in the other peloruside congeners, also suggests a δ-lactone in a boat conformation. This compound appears to be identical to *iso*-peloruside A, a side-product noted in Hoye's synthesis of **1**.[11]

Biogenesis and reactivity of the pelorusane scaffold

Compounds **3–6** shed light on the reactivity, possible biogenesis and biological importance of the SE corner (C-5 to C-9) of the pelorusane scaffold—including the pyran ring. With this albeit limited set of naturally occurring congeners, there is little evidence of variation in the PKS core gene cassette. While the C-7 acetal of peloruside D (**4**) could conceivably be the result of a skipped or missing ketoreductase step, it could also be the result of a subsequent oxidation, as shown in Scheme 2. All other differences, including *O*-methylation of C-3, C-7 and the oxidation state of C-8, are presumably the result of post-macrolactonisation modifications.

Peloruside D (**4**) provides an additional insight into the ease of formation of the pyran ring found in **1**, **2** and **3**, as it selects for the γ-pyrone given by the hemiacetal bridge between C-7 and C-11 in preference to the C-5 to C-9 acetal bridge found in the other pelorusides. To probe these observations, the energies of the epimeric acetals (7*R*-**4** and 7*S*-**4**) of peloruside D were calculated. In addition, the energies of the hypothetical alternative, peloruside A-like acetals (9*R*-**7** and 9*S*-**7**) of **4** (Fig. 9) were also calculated. Lowest energy conformers of these compounds were initially obtained using mixed torsional/low mode sampling conformational search as implemented in MacroModel[18] using the OPLS-2005 forcefield and a water continuum solvent model. The resultant structures were subjected to DFT B3LYP/6-31G** minimisations with aqueous solvation energies determined using the SM5.4 solvation model as implemented in Spartan '08.[19] The OPLS-2005 forcefield was chosen as it most reliably reproduces the lowest energy conformers of peloruside congeners found by DFT B3LYP/6-31G** minimisations. From these calculations, the 7*R*-**4** was more stable than the other possible acetals by between 14.5 and 82.6 kJ mol^{-1} (Table 5). Of particular note, the 7*R*-**4** is lower in energy than the peloruside A-like 9*R*-**7** by 37.4 kJ mol^{-1}. Molecular mechanics analysis of the 6-31-G** structures revealed that there is 34.6 kJ mol^{-1} higher torsional strain in 9*R*-**7** than that in 7*R*-**4** itself.

Table 5 Relative energies of different acetal forms of pelorusides A (**1**) and D (**4**)

Compound	Relative energy (kJ mol^{-1})
peloruside A (9*R*-**1**)	0[a]
9*S*-**1**	27.1[a]
keto-**1**	35.5[a]
peloruside D (7*R*-**4**)	0[b]
7*S*-**4**	14.5[b]
keto-**4**	58.1[b]
9*R*-**7**	37.2[b]
9*S*-**7**	82.6[b]

[a] Relative to 9*R*-**1**. [b] Relative to 7*R*-**4**.

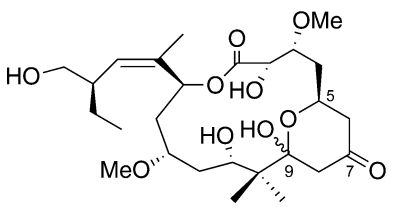

7

Fig. 9 Hypothetical peloruside A-like (C-5 to C-9) pyran isomer (**7**) of peloruside D.

The calculated energies in Table 5 led us to tentatively ascribe the stereochemistry of the C-7 acetal of peloruside D (**4**) as (*R*), with predicted energy differences between 7*R*-**4** and 7*S*-**4** of 14.5 kJ mol^{-1}. To validate this, the energies of peloruside A (**1**) and its corresponding (*S*)-acetal (9*S*-**1**) and pyran-lacking (*keto*-**1**) forms were determined as described above. These calculations showed the natural (*R*)-acetal of **1** to be favoured over the (*S*)-acetal by 27.1 kJ mol^{-1} and the *keto* form by 35.5 kJ mol^{-1}. It is interesting to note that although the *keto* form is predicted to have a significantly higher energy than the (*R*)-acetal from, we found NMR evidence of the *keto* form in the HMBC experiment (in $CDCl_3$ and C_6D_6), where it forms approximately 3% of peloruside A. This can be explained if the kinetics of the formation of the acetal are considerably slower than the kinetics of acetal opening. The *keto* form will also be more flexible than the acetal form, indicating an entropy penalty for acetal formation that will offset the enthalpic energies shown in Table 5.

The kinetic stability of *keto*-**1** is consistent with the preferential formation of the acetal of the C-7 and C-11 acetal of peloruside D (**4**) in preference to the C-5 to C-9 acetal bridge found in the other pelorusides. These results indicate that, although acetal formation is favoured, the acetal found in pelorusides A and B is difficult to form, and when a reasonable alternative becomes available it is preferred. This observation may be of significance for the design of synthetic approaches to peloruside A (**1**), its analogues and congeners.

A truncated version of **6**, corresponding to C-1 to C-6, was subjected to an exhaustive mixed torsional/low mode sampling conformational search as implemented in MacroModel using the OPLS-2005 forcefield and a chloroform continuum solvent model.

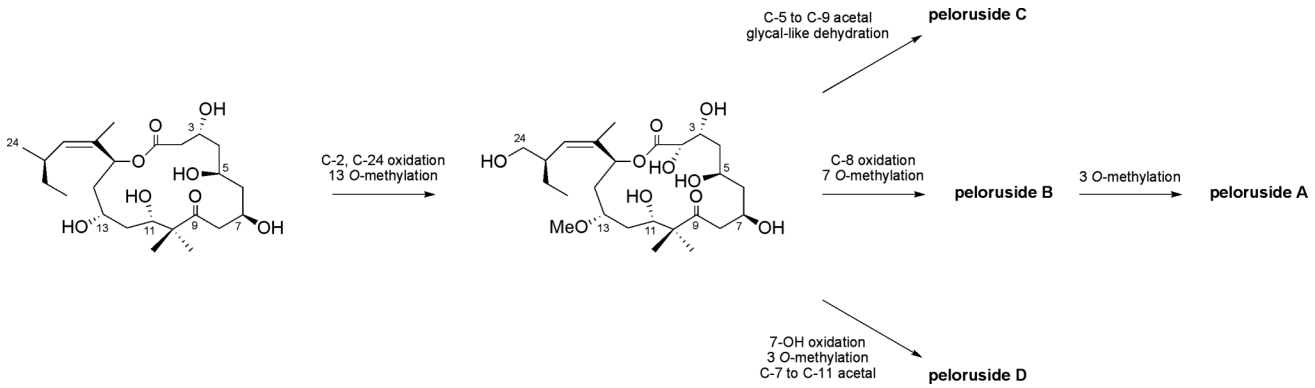

Scheme 2 Possible biogenesis of the pelorusides from a common precursor.

This showed that the boat conformer was more stable than the lowest energy chair conformer by 8.0 kJ mol^{-1}, primarily driven by reduced bond angle and torsional strains in the boat form compensating for a slightly increased energy relating to van der Waals interactions.

Biological activity

MTT cell proliferation assays[5] (96 h) against the human myeloid leukaemic (HL-60) cell line were performed for the two new peloruside congeners and the two semi-synthetic derivatives (**3**–**6**). Peloruside C (**3**) was found to be cytotoxic against the HL-60 cell line with an IC_{50} value of 221 nM, approximately 15 times less potent than **1** used in the same study (IC_{50} 15 nM). HL-60 and 1A9 (human ovarian carcinoma) cell lines treated with **3** at 660 nM were not significantly blocked at the G_2/M cell cycle checkpoint, with 13% of cells in G_2/M compared to 68% for peloruside A (**1**) and 20% for untreated control cells, as determined by flow cytometry.[5] In fact, an increase of cells in the G_1 phase was observed in the same assay for **3**, with 71% in G_1 compared to 54% in G_1 for untreated control cells and 13% in G_1 for cells treated with **1**. These results suggest the cytotoxicity displayed by compound **3** may not be related to the usual target of **1**, the mitotic microtubules. Peloruside D (**4**) and compounds **5** and **6** were only marginally active against the HL-60 cell line with IC_{50} values for cell growth inhibition of greater than 2 μM, 15 μM and 7 μM respectively. In paired tests, peloruside A inhibited cellular growth with an IC_{50} range of 10–35 nM. Because of the relatively weak cytotoxicities shown by these three compounds, they were not tested for cell cycle block using flow cytometry.

Despite its seemingly fragile chemical stability, it would seem that the C-5 to C-9 pyran is important for biological activity. Shortly after the initial report of **1**, we proposed that the C-5 to C-9 pyranose ring (now found to be present in **2**) was crucial for its cytotoxicity and microtubule-stabilising activity. The $NaBH_4$ reduction product **8** of peloruside A (Fig. 10), where the pyranose ring is irreversibly opened, showed a marked decrease (26-fold) in cytotoxicity.[2] The loss of activity on reduction of the pyranose ring presumably results from the markedly changed relative positioning of key tubulin-interacting functionalities across the peloruside-derived macrocycle subsequent to the loss of the pyran. The change from the C-5 to C-9 pyran of **1** to the C-7 to C-11 γ-pyrone moiety of **4** will have an equivalent effect, and the resultant loss of activity is expected. By contrast the differences between **1** and **3** are more subtle. There are four possible contributors to the resultant 15-fold reduction in activity: a) direct loss of key target interactions mediated by the C-8 and C-9 hydroxy groups and the methyl from the oxymethyl on C-7; b) conformational changes or solvation effects arising from the loss of intramolecular hydrogen bonds, for example between the hydroxy groups of C-9 and C-11 in **1**; c) loss of the hemiacetal of **1**, which has the potential to open and subsequently interact covalently with the target; and d) acquisition of a new target whose inhibition is less detrimental to cellular survival, a possibility that is consistent with the flow cytometry results shown above.

Recently, Altmann and co-workers reported the synthesis and biological testing of monocyclic peloruside analogue **9** (Fig. 10).[20] This compound was found to be several hundred-fold less potent than pelorusides A (**1**) or B (**2**) across a selection of cell lines, which correlates well with the lack of activity observed with the $NaBH_4$ reduction product of **1**. The lack of significant activity associated with trans-lactonisation product **6** also demonstrates that the macrocycle is also important for biological activity.

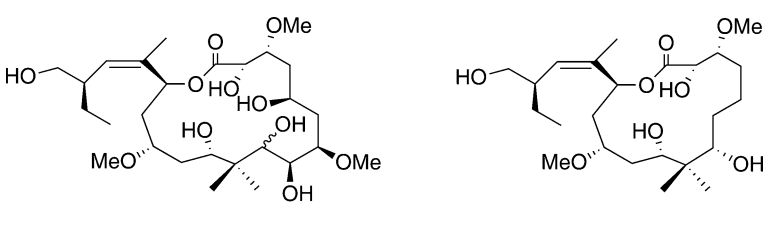

8 **9**

Fig. 10 Peloruside A reduction product (**8**) and Altmann's monocyclic peloruside analogue (**9**).

Conclusions

The combination of large-scale extraction of *Mycale hentscheli* and a structure-based assay has led to the identification of two new congeners (**3** and **4**) of peloruside A (**1**). Coupled with the semi-synthetic products **5** and **6**, we are able to further develop our understanding of the pharmacophore of this important class of tumour-suppressing macrolide. The new congeners and semi-synthetic derivatives reveal that peloruside A has a finely tuned pharmacophore, which is especially sensitive to modifications in the region of the pyran ring. Whilst formation of this important pyran is clearly favoured in **1** over the *keto* form, no reasonable alternative hemiacetal can be formed in this molecule. Where an alternative does exist (as in **4**), the C-5 to C-9 pyran is lost. In this way, mild disruptions to the structure of peloruside A can lead to dramatic loss of activity. This loss in activity is mirrored in the semi-synthetic products **5** and **6**, which are essentially inactive. Of the congeners presented here, the structural change in peloruside C (**3**) is the most subtle. However, we propose **3** interacts with a target other than tubulin, which has yet to be identified.

Experimental

General

NMR spectra were recorded on a Varian DirectDrive 600 MHz spectrometer equipped with a triple resonance HCN cryogenic probe, and a Varian Unity Inova Plus 500 MHz spectrometer. Chemical shifts δ (ppm) were referenced to the residual solvent peak.[21] High-resolution mass spectra were recorded using PE Biosystem Mariner 5158 TOF electrospray and Waters Q-TOF Premier Tandem spectrometers. Optical rotations were measured using a Perkin–Elmer 241 polarimeter. Normal-phase column chromatography was carried out using 2,3-dihydroxypropoxypropyl-derivatised silica (DIOL). Reversed-phase column chromatography was achieved using HP20 or HP20SS poly(styrene-divinylbenzene) (PSDVB) chromatographic resin. HPLC was performed using a Rainin Dynamax SD-200 solvent delivery system. Solvents used for normal- and reversed-phase column chromatography were of HPLC or analytical grade. All other solvents were purified by distillation. Solvent mixtures are reported as % vol/vol unless otherwise stated.

Animal material

Wild and aquacultured *Mycale hentscheli* specimens from Pelorus Sound, New Zealand were collected using SCUBA by Mike Page, National Institute of Water and Atmospheric Research (NIWA). Specimens were stored at –20 °C until required.

Isolation of pelorusides C and D

Frozen wild and aquacultured *Mycale hentscheli* (7.5 kg), from Pelorus Sound, New Zealand was cut into small pieces and steeped in MeOH (2 × 12 L) for 24 h. The methanolic extracts were loaded onto HP20 PSDVB beads, washed with H_2O and then eluted with i) 20% Me_2CO/H_2O, ii) 40% Me_2CO/H_2O, iii) 60% Me_2CO/H_2O and iv) Me_2CO. The 40% Me_2CO/H_2O fraction was then loaded onto HP20 PSDVB beads and eluted using MPLC and was eluted with increasing concentrations of Me_2CO in H_2O (20–100%). The 56–60% Me_2CO/H_2O fractions were combined and loaded onto HP20SS PSDVB beads and were eluted by MPLC with increasing concentrations of MeOH in H_2O (10–100%). The 75–100% $MeOH/H_2O$ fractions were combined, loaded onto a DIOL column, and eluted with portions of i) CH_2Cl_2 (fraction A), ii) 5% $MeCN/CH_2Cl_2$ (fraction B), iii) 10% $MeCN/CH_2Cl_2$ (fraction C) and iv) 50% $MeOH/CH_2Cl_2$ (fraction D). Fraction A yielded 60.7 mg of peloruside A (**1**). Fraction B (34.4 mg) was purified by HPLC (DIOL, 5 µm, 4.6 mm × 250 mm), with 20% *i*-PrOH/*n*-hexane as the mobile phase, yielding 23.9 mg of peloruside A (**1**) and 534 µg of peloruside D (**4**). Fraction C (5.4 mg) was loaded onto DIOL and eluted with increasing concentrations of MeCN in CH_2Cl_2 (1–10%), and 50% $MeOH/CH_2Cl_2$ to yield a colorless oil (3.0 mg). The resulting oil was purified by HPLC (DIOL, 5 µm, 4.6 mm × 250 mm), with 20% *i*-PrOH/*n*-hexane to yield 0.9 mg of peloruside A (**1**) and 130 µg of peloruside C (**3**).

Peloruside A (1). Colourless glass-like solid; NMR data see Table 2; all other data as previously published.[1]

Peloruside C (3). Colourless film; no optical rotation possible due to degradation of the compound; NMR data see Table 1; HRESIMS, $[M - H_2O + Na]^+$ observed *m*/*z* 491.26039, calculated 491.26154 for $C_{25}H_{40}O_8Na$, $\Delta = -2.3$ ppm.

Peloruside D (4). Colourless film; $[\alpha]_D^{25} - 4.5°$ (*c* 0.2, CH_2Cl_2); NMR data see Table 3; HRESIMS, $[M - H_2O + Na]^+$ observed *m*/*z* 521.27238, calculated 521.27211 for $C_{26}H_{42}O_9Na$, $\Delta = 0.5$ ppm.

Formation of hemiacetal (5)

To a solution of peloruside A (**1**, 0.5 mg, 0.91 µmol) in MeOH (150 µL) at room temperature was added 4 M aqueous HCl (150 µL). The reaction was stirred for 16 h and passed through a glass column packed with HP20SS (2 mL) pre-equilibrated in MeOH. The eluent was diluted with H_2O (1 mL) and passed through the column again. The eluent was further diluted with H_2O (2 mL) and passed through the column. The beads were then washed with H_2O (10 mL) and eluted with MeOH (10 mL). The crude methanolic fraction was concentrated to dryness *in vacuo* and was then purified by HPLC to give compound **5** (100 µg, 35% based on recovered starting material) and peloruside A (recovered, 200 µg) using the following conditions: 20% *i*-PrOH/*n*-hexane on DIOL (5 µm, 4.6 mm × 250 mm), 1 mL min^{-1}, 490 psi back pressure, detection at 210 nm. $[\alpha]_D$ +40.0° (*c* 0.01, CH_2Cl_2); NMR data see ESI;† HRESIMS, $[M - H_2O + Na]^+$ observed *m*/*z* 521.2731, calculated 521.2727 for $C_{26}H_{42}O_9Na$, $\Delta = -0.9$ ppm; IR (thin film) ν_{max} (cm^{-1}) 3360, 1764, 1726, 1462, 1276, 1261; R_t 5.2 min; R_f 0.50 (10% $MeOH/CH_2Cl_2$).

Formation of *seco*-peloruside A δ-lactone (6)

To a solution of peloruside A (**1**, 0.5 mg, 0.91 µmol) in CH_2Cl_2 (150 µL) at 0 °C was added TfOH (1 µL, 0.4 µmol) dropwise. The reaction was allowed to warm to room temperature slowly and stirred for 16 h. The reaction was quenched by the addition of MeOH (2 mL) and the solution was concentrated to half the volume *in vacuo*. The methanolic solution was passed through a glass column packed with HP20SS (2 mL) pre-equilibrated in MeOH. The eluent was diluted with H_2O (1 mL) and passed through the column again. The eluent was further diluted with

H_2O (2 mL) and passed through the column. The beads were then washed with H_2O (10 mL) and eluted with MeOH (10 mL). The crude methanolic fraction was concentrated to dryness *in vacuo* and was then purified by HPLC to give δ-lactone **6** (200 μg, 40%) using the following conditions: 15% *i*-PrOH/*n*-hexane on DIOL (5 μm, 4.6 mm × 250 mm), 1 mL min^{-1}, 610 psi back pressure, detection at 210 nm. $[\alpha]_D$ +150.0° (*c* 0.01, CH_2Cl_2); NMR data see ESI;† HRESIMS, $[M - H_2O + Na]^+$ observed 553.2994, calculated 553.2989 for $C_{27}H_{46}O_{10}Na$, $\Delta = -1.0$ ppm; IR (thin film) ν_{max} (cm^{-1}) 3439, 2956, 2925, 1738 (C═O), 1459, 1378, 1090; R_t 13.1 min; R_f 0.32 (5% MeOH/CH_2Cl_2).

Determination of biological activity

HL-60 human promyelocytic leukaemic cells were gifted from Dr Michael Berridge (Malaghan Institute of Medical Research, Wellington, New Zealand). 1A9 human ovarian carcinoma cells were gifted from Dr Paraskevi Giannakakou (Weill Cornell Medical College, NY, USA). The adherent 1A9 cells were detached with trypsin (0.05%) – ethylenediaminetetraacetic acid (EDTA, 0.53 mM) (Gibco-BRL, Invitrogen) and centrifuged at 300 × *g* to pellet cells and remove trypsin before re-suspension in fresh culture medium. All cells were grown at 37 °C in a 5% CO_2 in air atmosphere in RPMI-1640 medium (Gibco-BRL, Invitrogen) supplemented with 10% fetal calf serum (Gibco-BRL, Invitrogen) and 100 units mL^{-1} each of penicillin G and streptomycin sulfate (Gibco-BRL, Invitrogen). Cell culture medium for 1A9 cells also contained 0.25 units mL^{-1} insulin (Sigma–Aldrich, St. Louis, MO, USA). An MTT cell proliferation assay was used to assess the effect of the compounds on cell growth and viability. HL-60 cells were seeded at 1×10^4 cells per well in a 96-well plate and treated with test compound. After two days exposure, 20 μL of MTT (2-(4,5-dimethyl-2thiazolyl)-3,5-diphenyl-2H-tetrazolium bromide) solution (5 mg mL^{-1} in PBS) was added to each well. After two hours incubation at 37 °C, the blue formazan crystals that formed in viable cells were solubilised at 37 °C overnight in 100 μL 10% SDS, 45% dimethylformamide (pH 4.5). MTT reduction was measured the next day by absorbance at 570 nm in a multiwell plate reader (Versamax, Molecular Devices, Sunnyvale, CA). The MTT absorbance of individual wells was determined as a percent of control well absorbance. IC_{50} values were calculated using Sigma Plot software version 8 (Systat Software Inc., Point Richmond, CA, USA) and a four-parameter logistic curve.

Flow cytometry was used to determine the percentage of cells in different phases of the cell proliferation cycle. After treatment with test compound, HL-60 cells or detached 1A9 cells were suspended in 250 μL propidium iodide solution (0.05 mg mL^{-1} propidium iodide, 0.1% sodium citrate, 0.1% Triton X-100) for 15 min, and DNA content of individual cells was determined in a FACScan flow cytometer (Becton Dickinson, Franklin Lakes, NJ). Cell cycle analysis was performed using BD Cell Quest ™ Pro software (Becton Dickenson).

Computational details

Lowest energy conformers of the peloruside congeners studied were obtained by a combination of molecular mechanics and quantum mechanics methodology. Each structure was subjected to exhaustive conformational searching using the mixed torsional/low mode sampling routine as implemented in MacroModel version 9.7 and visualised in Maestro 9.0. A minimum of 70 000 steps were applied, and structures obtained were minimised using the OPLS_2005 forcefield using the GB/SA water continuum solvent model[22] and the Polak–Ribiere conjugate gradient (PRCG) conjugate gradients method and terminated on a gradient threshold of 0.005 kJ $mol^{-1}Å^{-1}$. The simulation was repeated until the lowest energy structure reported had been replicated at least 100 times. Lowest energy structures were then subjected to equilibrium geometry optimisation using the B3LYP hybrid density functional method[23,24] and the 6-31G** basis set in Spartan '08. Aqueous solvation energies were determined using the SM5.4 model.[25]

Acknowledgements

The authors thank Mike Page and Sean Handley of the National Institute of Water and Atmospheric Research (NIWA) and Izabela Pomer (VUW) for sponge aquaculture, collection and processing. Dr John Ryan (VUW) for NMR assistance. We acknowledge the Foundation for Research, Science & Technology (FRST) and the Curtis-Gordon Research Scholarship in Chemistry (A.J.S.), and the Tertiary Education Commission of New Zealand (M.R.) for funding. We also thank the Wellington Medical Research Foundation and VUW Postgraduate Research Scholarship for funding (T.N.G., A. W.).

References

1 L. M. West, P. T. Northcote and C. N. Battershill, *J. Org. Chem.*, 2000, **65**, 445–449.
2 K. A. Hood, L. M. West, B. Rouwé, P. T. Northcote, M. V. Berridge, S. J. Wakefield and J. H. Miller, *Cancer Res.*, 2002, **62**, 3356–3360.
3 T. N. Gaitanos, R. M. Buey, J. F. Díaz, P. T. Northcote, P. Teesdale-Spittle, J. M. Andreu and J. H. Miller, *Cancer Res.*, 2004, **64**, 5063–5067.
4 E. Hamel, B. W. Day, J. H. Miller, M. K. Jung, P. T. Northcote, A. K. Ghosh, D. P. Curran, M. Cushman, K. C. Nicolaou, I. Paterson and E. J. Sorensen, *Mol. Pharmacol.*, 2006, **70**, 1555–1564.
5 A. Wilmes, K. Bargh, C. Kelly, P. T. Northcote and J. H. Miller, *Mol. Pharmaceutics*, 2007, **4**, 269–280.
6 X. Liao, Y. Wu and J. K. De Brabander, *Angew. Chem., Int. Ed.*, 2003, **42**, 1648–1652.
7 M. Jin and R. E. Taylor, *Org. Lett.*, 2005, **7**, 1303–1305.
8 A. K. Ghosh, X. Xu, J.-H. Kim and C.-X. Xu, *Org. Lett.*, 2008, **10**, 1001–1004.
9 D. A. Evans, D. S. Welch, A. W. H. Speed, G. A. Moniz, A. Reichelt and S. Ho, *J. Am. Chem. Soc.*, 2009, **131**, 3840–3841.
10 M. A. McGowan, C. P. Stevenson, M. A. Schiffler and E. N. Jacobsen, *Angew. Chem., Int. Ed.*, 2010, **49**, 6147–6150.
11 T. R. Hoye, J. Jeon, L. C. Kopel, T. D. Ryba, M. A. Tennakoon and Y. Wang, *Angew. Chem., Int. Ed.*, 2010, **49**, 6151–6155.
12 S. M. Dalby and I. Paterson, *Curr. Opin. Drug Discovery Devel.*, 2010, **13**, 777–794.
13 A. J. Singh, C.-X. Xu, X. Xu, L. M. West, A. Wilmes, A. Chan, E. Hamel, J. H. Miller, P. T. Northcote and A. K. Ghosh, *J. Org. Chem.*, 2010, **75**, 2–10.
14 M. J. Page, P. T. Northcote, V. L. Webb, S. Mackey and S. J. Handley, *Aquaculture*, 2005, **250**, 256–269.
15 M. Page, L. West, P. Northcote, C. Battershill and M. Kelly, *J. Chem. Ecol.*, 2005, **31**, 1161–1174.
16 B. Pera, M. Razzak, C. Trigili, O. Pineda, A. Canales, R. M. Buey, J. Jiménez-Barbero, P. T. Northcote, I. Paterson, I. Barasoain and J. F. Díaz, *ChemBioChem*, 2010, **11**, 1669–1678.
17 An alternative pathway for this transformation based on a pinacol rearrangement was suggested by a reviewer. However, due to the presumed ease of β-elimination of the C-7 methoxy group in the presence of the C-9 ketone, we favour the pathway shown in Scheme 1.

18 F. Mohamadi, N. G. J. Richards, W. C. Guida, R. Liskamp, M. Lipton, C. Caufield, G. Chang, T. Hendrickson and W. C. Still, *J. Comput. Chem.*, 1990, **11**, 440–467.
19 Y. Shao, L. F. Molnar, Y. Jung, J. Kussmann, C. Ochsenfeld, S. T. Brown, A. T. B. Gilbert, L. V. Slipchenko, S. V. Levchenko, D. P. O'Neill, R. A. DiStasio Jr, R. C. Lochan, T. Wang, G. J. O. Beran, N. A. Besley, J. M. Herbert, C. Yeh Lin, T. Van Voorhis, S. Hung Chien, A. Sodt, R. P. Steele, V. A. Rassolov, P. E. Maslen, P. P. Korambath, R. D. Adamson, B. Austin, J. Baker, E. F. C. Byrd, H. Dachsel, R. J. Doerksen, A. Dreuw, B. D. Dunietz, A. D. Dutoi, T. R. Furlani, S. R. Gwaltney, A. Heyden, S. Hirata, C.-P. Hsu, G. Kedziora, R. Z. Khalliulin, P. Klunzinger, A. M. Lee, M. S. Lee, W. Liang, I. Lotan, N. Nair, B. Peters, E. I. Proynov, P. A. Pieniazek, Y. Min Rhee, J. Ritchie, E. Rosta, C. David Sherrill, A. C. Simmonett, J. E. Subotnik, H. Lee Woodcock III, W. Zhang, A. T. Bell, A. K. Chakraborty, D. M. Chipman, F. J. Keil, A. Warshel, W. J. Hehre, H. F. Schaefer III, J. Kong, A. I. Krylov, P. M. W. Gill and M. Head-Gordon, *Phys. Chem. Chem. Phys.*, 2006, **8**, 3172–3191.
20 C. W. Wullschleger, J. Gertsch and K.-H. Altmann, *Org. Lett.*, 2010, **12**, 1120–1123.
21 H. E. Gottlieb, V. Kotlyar and A. Nudelman, *J. Org. Chem.*, 1997, **62**, 7512–7515.
22 W. C. Still, A. Tempczyk, R. C. Hawley and T. Hendrickson, *J. Am. Chem. Soc.*, 1990, **112**, 6127–6129.
23 A. D. Becke, *J. Chem. Phys.*, 1993, **98**, 5648–5652.
24 C. Lee, W. Yang and R. G. Parr, *Phys. Rev. B: Condens. Matter*, 1988, **37**, 785–789.
25 C. C. Chambers, G. D. Hawkins, C. J. Cramer and D. G. Truhlar, *J. Phys. Chem.*, 1996, **100**, 16385–16398.

